

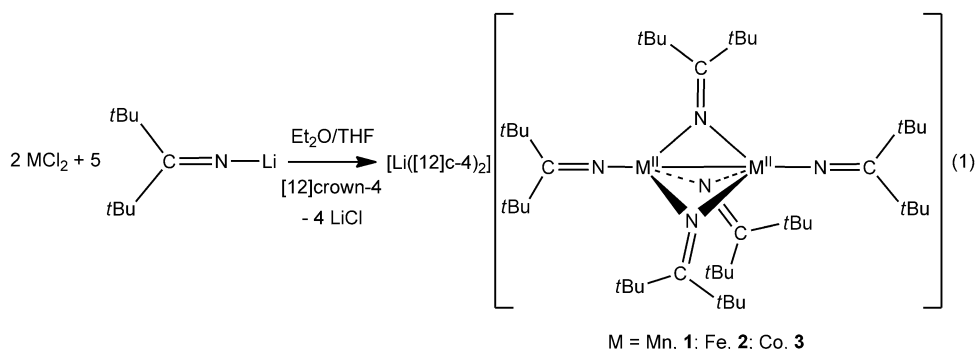
Synthesis and Characterization of $[M_2(N=CtBu_2)_5]^-$ ($M = Mn, Fe, Co$): Metal Ketimide Complexes with Strong Metal–Metal Interactions**

Richard A. Lewis, Simona Morochnik, Alon Chapovetsky, Guang Wu, and Trevor W. Hayton*

The study of metal–metal interactions has provided many important insights into transition-metal bonding and electronic structure.^[1] This is perhaps best exemplified by the synthesis of quintuply bonded $[Ar'CrCrAr']$ ($Ar' = C_6H_5-2,6(C_6H_3-2,6-iPr_2)_2$), which has intrigued both experimentalists and theoreticians since it was first reported in 2005.^[2] Complexes with metal–metal bonds also exhibit interesting optoelectronic properties^[2d] and intriguing chemical reactivity.^[3] Interestingly, a survey of complexes with metal–metal bonds shows a large knowledge gap between the late first-row transition metals and the rest of the transition-metal block. For example, the Cambridge Structural Database contains only a few M_2^{4+} complexes with metal–metal bonds for Mn (4 structures), Fe (28 structures), and Co (54 structures),^[4] whereas many more structure are known for Cr (> 500 structures), Ru (> 500), and Rh (> 1500 structures).^[1] These trends can be rationalized by the contracted nature of the 3d electrons for the later first-row transition metals,^[2i] and highlights the challenge of making metal–metal bonds with these elements. In this regard, the development of new ligands that can promote metal–metal bonding would be of significant benefit for the exploration of these interactions and their application in the field of catalysis. Herein we demonstrate the ability of the ketimide ligand, $[N=CR_2]^-$,^[5] to promote metal–metal interactions, specifically in the ketimide-bridged transition-metal complexes, $[M_2(N=CtBu_2)_5]^-$ ($M = Mn, Fe, Co$), which exhibit short metal–metal distances and strong inter-metal magnetic communication.

Addition of 2.5 equiv of $Li(N=CtBu_2)$ to MCl_2 ($M = Mn, Fe, \text{ and } Co$) in THF, followed by addition of 1 equiv of

$[12]crown-4$, provides $[Li([12]crown-4)_2][M_2(N=CtBu_2)_5]$ ($M = Mn, 1; Fe, 2; Co, 3$) in 58–78% yield [Eq. (1)]. Complexes **1–3** crystallize in the monoclinic space group $C2/c$ as discrete cation–anion pairs. Each complex features



two terminal ketimide ligands and three bridging ketimide ligands, resulting in the formation of two co-facial tetrahedra (Figure 1). The M–N bond lengths of the bridging ketimide ligands (Mn 2.142(3)–2.149(2) Å, Fe 2.044(4)–2.072(4) Å, Co 2.018(2)–2.055(2) Å), are consistent with previously reported values for μ -($N=CtBu_2$) interactions,^[5b] while the M–N–M angles (Mn 74.46(8)–74.6(1)°, Fe 72.8(1)–73.1(2)°, Co 71.8(1)–72.82(7)°), are smaller than those observed previously.^[5b] As anticipated, the M–N bond lengths for the terminal ketimide ligands are shorter than the bridging ketimide M–N bond lengths (Mn 1.971(2) Å, Fe 1.894(4) Å, Co 1.844(2) Å). Interestingly, the terminal Mn–N bond length for **1** is 0.1 Å longer than that exhibited by the related Mn^{II} ketimide, $[Mn_3(N=CtBu_2)_6]$,^[5b] which does not possess a metal–metal bond (Mn1–Mn2 2.8183(8) Å), suggesting the presence of a trans influence from the Mn–Mn interaction in **1** (see below).

The most notable structural features for complexes **1–3** are the M–M distances (Mn 2.5965(7) Å, Fe 2.443(1) Å, Co 2.4097(7) Å). These M–M distances are amongst the shortest reported for late first-row transition-metal complexes with an M_2^{4+} core,^[6] and in the case of **2** and **3**, are suggestive of an M–M bond.^[2b] For comparison, the isostructural thiolates $[M_2(SR)_5]^-$ feature longer M–M distances,^[7] ranging from 2.491(1) Å ($M = Co, R = iPr$) to 2.634(1) Å ($M = Fe, R = iPr$) and 2.607(3) Å ($M = Ni, R = 2,4,6-iPr_3C_6H_2$).^[8] Furthermore, the Fe^I dimer $[Ar'FeFeAr']$ exhibits a Fe–Fe distance of 2.5151(9) Å,^[2b] while the Fe_2^{3+} complex $[Fe_2(DPhF)_3]$ (DPhF = diphenylforamidinate) has an Fe–Fe bond length of 2.2318(8) Å.^[9] Both complexes are thought to feature direct Fe–Fe bonds. Finally, the Co_2^{4+} complex $[Co_2(DPhF)_3]^-$

[*] R. A. Lewis, S. Morochnik, A. Chapovetsky, G. Wu, Prof. T. W. Hayton
Department of Chemistry and Biochemistry
University of California Santa Barbara
Santa Barbara, CA 93106 (USA)
E-mail: hayton@chem.ucsb.edu

[**] We thank the National Science Foundation (CHE 1059097) and Alfred P. Sloan Foundation for financial support of this work. We also thank Prof. Matt Shores for helpful discussions. This research made use of the SQUID Magnetometer of the Materials Research Laboratory: an NSF MRSEC, supported by NSF DMR 1121053.

Supporting information for this article is available on the WWW under <http://dx.doi.org/10.1002/anie.201206790>.

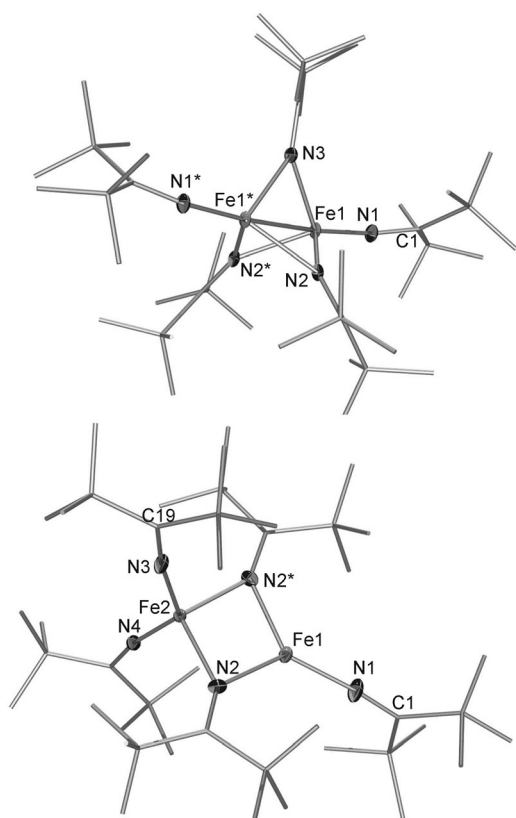


Figure 1. ORTEP drawings of complex **2** (above) and **4** (below) with ellipsoids for non-carbon atoms set at 50%. Hydrogen atoms and the $[\text{Li}([12]\text{crown-4})_2]^+$ ion have been omitted for clarity.

$(\text{MeCN})_2][\text{PF}_6]$ has a $\text{Co}\cdots\text{Co}$ distance of $2.885(1) \text{ \AA}$,^[10] indicating that no direct Co-Co bond is present.

We endeavored to probe the magnetic properties of complexes **1–3** to gain additional insight into the nature of the short metal–metal distances observed in the solid state. Complex **1** exhibits an observed effective magnetic moment of 3.85 B.M. at 300 K; this drops precipitously to 0.54 B.M. at 4 K (Figure 2). The low value at 4 K suggests that all ten

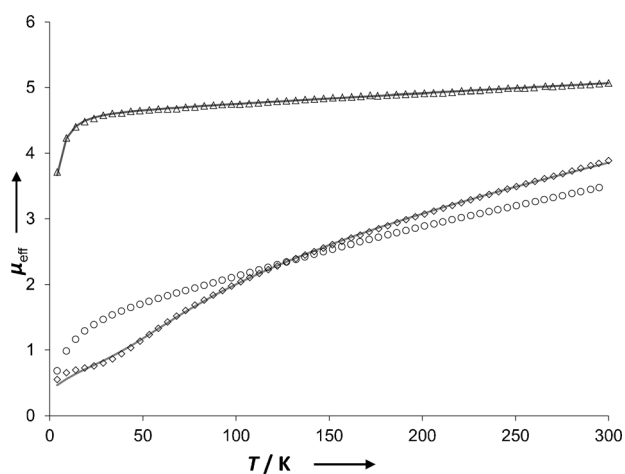


Figure 2. Solid-state magnetic susceptibility data (μ_{eff} vs. T) for **1** (\diamond), **2** (\triangle), and **3** (\circ) measured from 300 K to 4 K.

d electrons within the Mn_2^{4+} core are antiferromagnetically coupled, essentially resulting in a diamagnetic ground state at low temperatures. To fit the magnetic data, we used the exchange Hamiltonian $\hat{H} = -2J\hat{S}_{\text{Mn}}\hat{S}_{\text{Mn}}$, with $S_1 = S_2 = 5/2$.^[11] The data were fitted with $J = -78 \text{ cm}^{-1}$, $g_1 = g_2 = 2.025$, $D_1 = D_2 = -12.64 \text{ cm}^{-1}$, and 0.4 % paramagnetic impurity ($S = 5/2$). The large J value supports strong antiferromagnetic coupling between Mn centers. Complex **2** exhibits an observed effective magnetic moment of 5.06 B.M. at 300 K, which drops slightly to 3.72 B.M. at 4 K (Figure 2). Complex **2**, with its shorter M–M distance, could not be reasonably modeled by assuming $S_1 = S_2 = 2$. However, a good fit could be achieved with $S_1 = S_2 = 1$, $J = 2.24 \text{ cm}^{-1}$, $g_1 = g_2 = 2.302$, $D_1 = D_2 = -0.002 \text{ cm}^{-1}$, and $\text{TIP} = 1.87 \times 10^{-3} \text{ cm}^3 \text{ mol}^{-1}$ (see the Supporting Information). The overall $S = 2$ spin state at 300 K indicates that four electrons within the Fe_2^{4+} core are strongly antiferromagnetically coupled at this temperature, possibly by two metal–metal bonding interactions. Additionally, the fit suggests the presence of weak ferromagnetic coupling between the remaining unpaired d electrons. In comparison, the iminoacyl-bridged Fe_2^{4+} dimer $[\{\text{Fe}(\text{C}(\text{Mes})=\text{N}t\text{Bu})_2\}_2]$ ($\text{Mes} = 2,4,6\text{-Me}_3\text{C}_6\text{H}_2$) was modeled with an $S_1 = S_2 = 3/2$ ground state,^[12] which Floriani and co-workers argued was evidence for an Fe–Fe single bond. Finally, complex **3** has an observed effective magnetic moment of 3.50 B.M. at 300 K, which drops to 0.68 B.M. at 4 K (Figure 2). Unfortunately, the magnetic data could not be reasonably modeled with the simple spin-exchange Hamiltonian used for **1** and **2**. Nonetheless, it is clear that complex **3** also exhibits strong magnetic communication between metal centers.

Recently, Lu et al. calculated a $(\sigma)^2(\pi)^4(\pi^*)^2(\sigma^*)^1(\delta)^2(\delta^*)^2$ electronic configuration for C_3 symmetric $[\text{Fe}_2(\text{DPhF})_3]$,^[9] which accounts for its $S = 7/2$ ground state and predicts a Fe–Fe bond order of 1.5 (ignoring multiconfigurational effects). Similarly, a $(\sigma)^2(\pi)^4(\sigma^*)^2(\pi^*)^2(\delta)^2(\delta^*)^0$ electronic configuration for **2** could account for its $S = 2$ ground state, and suggest a Fe–Fe bond order of 2. The switch in σ^* and π^* orbital ordering in **2**, relative to $[\text{Fe}_2(\text{DPhF})_3]$, can be explained by invoking strong π -donation from the terminal ketimide ligands, which would tend to destabilize the π -symmetry orbitals relative to those with σ symmetry.

Complexes **1–3** are insoluble in hexanes and benzene, but are quite soluble in Et_2O , THF, and pyridine. Interestingly, the ^1H and ^7Li NMR spectra of **1** and **2** are more complicated than the solid-state structures would suggest. For example, the ^7Li NMR spectrum of **2** in $[\text{D}_8]\text{THF}$ at room temperature consists of a broad singlet -238 ppm . The large upfield shift is indicative of an interaction between the Li and the paramagnetic Fe centers. On cooling to -40°C , this resonance shifts to -352 ppm , while a new resonance at 0.49 ppm , assignable to $[\text{Li}([12]\text{crown-4})_2]^+$, appears in the spectrum (see the Supporting Information). The ^7Li NMR spectra of **1** in $[\text{D}_5]\text{pyridine}$ are also indicative of fluxional behavior. Overall, the ^7Li NMR data of **1** and **2** suggest the presence of an equilibrium between $[\text{Li}([12]\text{crown-4})_2][\text{M}_2(\text{N}=\text{CrBu}_2)_5]$ and a close-contact ion pair. On cooling, Li exchange is slowed and resonances attributable to both species are observable. In contrast to the NMR data collected for **1** and **2**, the ^1H and ^7Li NMR spectra for **3** are relatively

straightforward. The ^1H NMR spectrum of **3** in $[\text{D}_5]\text{pyridine}$ at room temperature consists of a broad singlet at 30.69 ppm, assignable to the *tert*-butyl groups of the ketimide ligands (see the Supporting Information), while the ^7Li NMR spectrum of **3** consists of a sharp singlet at 3.80 ppm, assignable to the $[\text{Li}([12]\text{crown-4})_2]^+$ ion.

To further probe the solution phase structures of **1–3** in donor solvents, we performed magnetization experiments according to Evans' method. Complex **1** exhibits a room temperature magnetic moment of 6.9 B.M. in $[\text{D}_5]\text{pyridine}$. This value is substantially larger than that observed in the solid state, suggesting that there is less magnetic interaction between Mn^{2+} centers in **1** in the solution phase. Similarly, complexes **2** and **3** exhibit room temperature moments of 6.6 B.M. and 5.3 B.M., respectively. Again, these values are larger than those recorded in the solid state, and are suggestive of a structural change in solution. Based on the VT NMR experiments (see above), we postulate that coordination of Li^+ into the secondary coordination sphere weakens the M–M interaction, resulting in a decrease in the antiferromagnetic coupling.

We also explored the redox chemistry of complex **2**. The cyclic voltammogram of **2** in THF reveals a reversible oxidation feature at -0.43 V (vs. Fc/Fc^+), assignable to the formation of an $\text{Fe}^{\text{III}}/\text{Fe}^{\text{II}}$ dimer. Consistent with cyclic voltammetry results, chemical oxidation of **2** with 0.5 equiv of I_2 in Et_2O , results in the generation of $[\text{Fe}_2(\text{N}=\text{C}t\text{Bu}_2)_5]$ (**4**) [Eq. (2)], which is isolable as a deep-maroon crystalline solid in 45% yield. The ^1H NMR spectrum in C_6D_6 consists of a broad singlet centered at 10.6 ppm, which is assignable to the *tert*-butyl groups of the ketimide ligands.

Complex **4** crystallizes in the orthorhombic space group *Pnma*. Interestingly, **4** is not isostructural with complexes **1–3** (Figure 1). Instead, its structure consists of a tetrahedral Fe^{3+} ion connected to a trigonal planar Fe^{2+} center by only two bridging ketimide ligands. The Fe–Fe distance in **4** (2.5468(14) Å) is 0.10 Å longer than that observed in **2**. This lengthening may be attributable to a reduction in the M–M bond order upon oxidation. Despite this difference, the Fe–N bond lengths of the bridging ketimide ligands in **4** (1.991(4)–2.014(4) Å) are still comparable to those observed for **2**.

The solid-state magnetic susceptibility of **4** was determined by SQUID magnetometry (see the Supporting Information). As seen for complexes **1–3**, compound **4** exhibits evidence for strong magnetic communication between metal

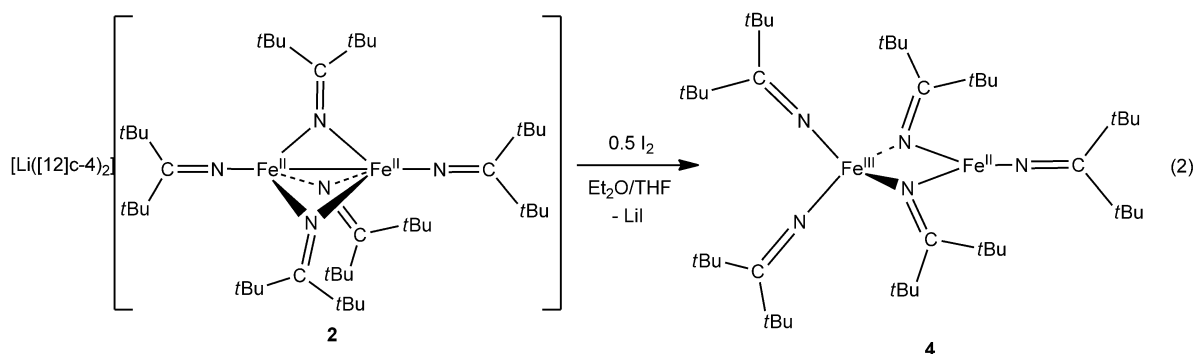
centers. Complex **4** has an observed effective magnetic moment of $\mu_{\text{eff}} = 4.01\text{ B.M.}$ at 300 K, which drops to 2.40 B.M. at 5 K. The data were fitted with $S_1 = 5/2$, $S_2 = 2$, $J = -235\text{ cm}^{-1}$, $g_1 = 4.518$, $g_2 = 5.772$, $D_1 = -0.443\text{ cm}^{-1}$, and $D_2 = -0.023\text{ cm}^{-1}$. While the fit is not as satisfactory as those achieved for complexes **1** and **2**, several important conclusions can still be drawn. In particular, the overall $S = 9/2$ spin state for **4**, versus the $S = 2$ spin state of **2**, suggest the absence of a direct Fe–Fe bond, which is consistent with the longer Fe–Fe bond length found in the solid state for **4**. However, the large J value still reveals strong antiferromagnetic coupling between the two Fe centers, most likely by a super-exchange mechanism.

In summary, we have isolated a series of ketimide-bridged dimers, $[\text{Li}([12]\text{crown-4})_2][\text{M}_2(\text{N}=\text{C}t\text{Bu}_2)_5]$ ($\text{M} = \text{Mn}, \text{Fe}, \text{Co}$). These complexes exhibit short metal–metal distances and strong electronic communication between metal centers, as revealed by X-ray crystallography and SQUID magnetometry, respectively. Comparably strong metal–metal interactions are rare in these elements. Indeed, magnetic susceptibility measurements support the presence of a direct M–M bond in the iron analogue. This work demonstrates that the ketimide ligand is capable of promoting strong metal–metal interactions, most likely because of its strong π -donating ability,^[5c] and should be considered a viable co-ligand for future research on metal–metal bonding. Additionally, its ability to adopt multiple coordination modes presents opportunities for ligand architectures not possible with other metal–metal bond-promoting ligands.^[13] We will continue to investigate the electronic structures of these ketimide complexes and further explore the ability of the ketimide ligand to produce multimetallic complexes.

Received: August 22, 2012

Published online: November 7, 2012

Keywords: ketimides · magnetism · metal–metal interactions · transition metals



- Long, M. Brynda, P. P. Power, *Angew. Chem.* **2008**, *120*, 9255–9257; *Angew. Chem. Int. Ed.* **2008**, *47*, 9115–9117; c) G. La Macchia, L. Gagliardi, P. P. Power, M. Brynda, *J. Am. Chem. Soc.* **2008**, *130*, 5104–5114; d) G. Li Manni, A. L. Dzubak, A. Mulla, D. W. Brogden, J. F. Berry, L. Gagliardi, *Chem. Eur. J.* **2012**, *18*, 1737–1749; e) H. Lei, J.-D. Guo, J. C. Fetting, S. Nagase, P. P. Power, *J. Am. Chem. Soc.* **2010**, *132*, 17399–17401; f) R. Wolf, C. Ni, T. Nguyen, M. Brynda, G. J. Long, A. D. Sutton, R. C. Fischer, J. C. Fetting, M. Hellman, L. Pu, P. P. Power, *Inorg. Chem.* **2007**, *46*, 11277–11290; g) J. Huang, Q. X. Li, H. Ren, H. B. Su, J. L. Yang, *J. Chem. Phys.* **2006**, *125*, 1–4; h) M. Brynda, L. Gagliardi, P. O. Widmark, P. P. Power, B. O. Roos, *Angew. Chem.* **2006**, *118*, 3888–3891; *Angew. Chem. Int. Ed.* **2006**, *45*, 3804–3807; i) B. O. Roos, A. C. Borin, L. Gagliardi, *Angew. Chem.* **2007**, *119*, 1491–1494; *Angew. Chem. Int. Ed.* **2007**, *46*, 1469–1472; j) G. Merino, K. J. Donald, J. S. D'Acchioli, R. Hoffmann, *J. Am. Chem. Soc.* **2007**, *129*, 15295–15302; k) R. Ponc, F. Feixas, *J. Phys. Chem. A* **2009**, *113*, 8394–8400; l) G. La Macchia, G. L. Manni, T. K. Todorova, M. Brynda, F. Aquilante, B. O. Roos, L. Gagliardi, *Inorg. Chem.* **2010**, *49*, 5216–5222.
- [3] a) D. J. Timmons, M. P. Doyle in *Multiple Bonds Between Metal Atoms*, 3rd ed. (Eds.: F. A. Cotton, C. A. Murillo, R. A. Walton), Springer Science, New York, **2005**, pp. 591–632; b) A. F. Heyduk, D. G. Nocera, *Science* **2001**, *293*, 1639–1641; c) M. H. Chisholm, *Acc. Chem. Res.* **1990**, *23*, 419–425.
- [4] Cambridge Structural Database. version 1.14 ed., **2012**.
- [5] a) R. A. Lewis, G. Wu, T. W. Hayton, *J. Am. Chem. Soc.* **2010**, *132*, 12814–12816; b) R. A. Lewis, G. Wu, T. W. Hayton, *Inorg. Chem.* **2011**, *50*, 4660–4668; c) R. A. D. Soriaga, J. M. Nguyen, T. A. Albright, D. M. Hoffman, *J. Am. Chem. Soc.* **2010**, *132*, 18014–18016.
- [6] S. Kuppuswamy, M. W. Bezpalko, T. M. Powers, M. M. Turnbull, B. M. Foxman, C. M. Thomas, *Inorg. Chem.* **2012**, *51*, 8225–8240.
- [7] a) G. Henkel, C. Chen, *Inorg. Chem.* **1993**, *32*, 1064–1065; b) G. Henkel, S. Weissgräber, *Angew. Chem.* **1992**, *104*, 1382–1383; *Angew. Chem. Int. Ed. Engl.* **1992**, *31*, 1368–1369; c) K. Ruhlandt-Senge, P. P. Power, *J. Chem. Soc. Dalton Trans.* **1993**, 649–650.
- [8] A. Silver, M. Millar, *J. Chem. Soc. Chem. Commun.* **1992**, 948–949.
- [9] C. M. Zall, D. Zhrebetskyy, A. L. Dzubak, E. Bill, L. Gagliardi, C. C. Lu, *Inorg. Chem.* **2012**, *51*, 728–736.
- [10] F. A. Cotton, L. M. Daniels, D. J. Maloney, J. H. Matonic, C. A. Murillo, *Inorg. Chim. Acta* **1997**, *256*, 283–289.
- [11] E. Bill, *julX*, version 1.4.1 ed., Muelheim/Ruhr, **2008**.
- [12] A. Klose, E. Solari, C. Floriani, A. Chiesi-Villa, C. Rizzoli, N. Re, *J. Am. Chem. Soc.* **1994**, *116*, 9123–9135.
- [13] J. P. Krogman, B. M. Foxman, C. M. Thomas, *J. Am. Chem. Soc.* **2011**, *133*, 14582–14585.